J. Fluid Mech. (2019), *vol.* 868, R4, doi:10.1017/jfm.2019.214

JFM RAPIDS
journals.cambridge.org/rapids

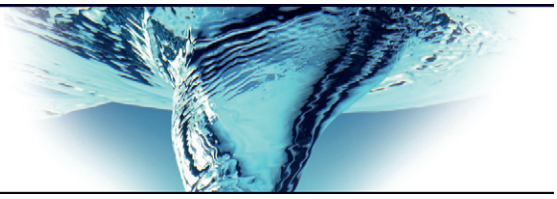

Subharmonic edge wave excitation by narrow-band, random incident waves

Giovanna Vittori[1,†], Paolo Blondeaux[1], Giovanni Coco[2] and R. T. Guza[3]

[1]Department of Civil, Chemical and Environmental Engineering, University of Genoa, Via Montallegro 1, 16145 Genova, Italy

[2]School of Environment, University of Auckland, 1010 Auckland, New Zealand

[3]Integrative Oceanography Division – Scripps Institution of Oceanography, University of California, La Jolla, CA 92093-0209, USA

(Received 23 December 2018; revised 27 February 2019; accepted 12 March 2019; first published online 12 April 2019)

A monochromatic, small amplitude, normally incident standing wave on a sloping beach is unstable to perturbation by subharmonic (half the frequency) edge waves. At equilibrium, edge wave shoreline amplitudes can exceed incident wave amplitudes. Here, the effect of incident wave randomness on subharmonic edge wave excitation is explored following a weakly nonlinear stability analysis under the assumption of narrow-band incident random waves. Edge waves respond to variations in both incident wave phase and amplitude, and the edge wave amplitudes and incident wave groups vary on similar time scales. When bottom friction is included, intermittent subharmonic edge wave excitation is predicted due to the combination of bottom friction and wave phase. Edge wave amplitude can be near zero for long times, but for short periods reaches relatively large values, similar to amplitudes with monochromatic incident waves and no friction.

Key words: coastal engineering, surface gravity waves

1. Introduction

Edge waves are surface gravity waves trapped by refraction at the shoreline of a sloping beach. Edge waves vary sinusoidally in the alongshore direction and their amplitude decreases in the offshore direction. Despite extensive study and speculation, edge wave dynamics and its role in nearshore processes remains poorly understood. Mechanisms proposed to excite edge waves include wind blowing along the coast, pressure variations induced by storms travelling parallel to the coast (Greenspan 1956; Munk & Carrier 1956), storm surges, tsunamis (Bricker *et al.* 2007) and groups of wind waves (Gallagher 1971).

† Email address for correspondence: vittori@dicat.unige.it

Moreover, edge waves can form because of the instability of nearly monochromatic waves which normally approach a reflective beach. The phenomenon can be modelled by means of the shallow water continuity and momentum equations which describe an irrotational standing wave on a plane beach and can be solved exactly with a hodographic transformation (Carrier & Greenspan 1958). However, as shown by Guza & Davis (1974), a standing wave on a plane longshore uniform beach is unstable to perturbation by subharmonic edge waves. Galvin (1965) and Harris (1967) first observed the instability in a laboratory wave basin. Later laboratory experiments (Guza & Inman 1975; Yeh 1986; Buchan & Pritchard 1995), using monochromatic wave forcing, confirmed the original theory (Guza & Davis 1974). More recent laboratory experiments investigated the effect of spectral forcing (Ding *et al.* 2018) and wave breaking (Abcha *et al.* 2017) on the formation of edge waves. The monochromatic theory was later extended to allow different cross-shore bottom profiles and to include nonlinear effects that limit edge wave growth (e.g. Guza & Bowen 1976; Minzoni & Whitham 1977; Rockliff 1978; Mei 1989; Johnson 2005; Li 2007).

Natural ocean waves are random and can be described as the superposition of different harmonic components. Vittori & Blondeaux (1997) considered edge waves generated through nonlinear instability by random incident waves characterized by a narrow-band spectrum. They found that the effect of the random incident wave is that of widening the unstable regions in the parameter space and decreasing the equilibrium amplitude of the edge waves, as the width of the spectrum is increased. Here, we explore theoretically the combined effect of incident wave randomness and dissipative effects on subharmonic edge wave excitation, building on Vittori & Blondeaux (1997). Incoming surface waves are assumed to have a narrow-band spectrum, and the solution is determined numerically.

The next sections provide the formulation of the problem and the main steps to derive the equation describing the time development of the edge wave amplitude. We then present and discuss the results, while the last section is devoted to the conclusions.

2. Incident wave and edge wave definition

2.1. *Incident waves*

In a weakly nonlinear expansion of a standing wave on a plane, longshore uniform beach, the non-dimensional shoreline amplitude a is defined as

$$a = \frac{a^* \omega_0^{*2}}{g^* s^2} \ll 1, \tag{2.1}$$

where a^* is the dimensional amplitude of the wave at the shoreline, ω_0^* is its angular frequency, g^* is gravity, s is the beach slope and * indicates dimensional variables. Following Vittori & Blondeaux (1997), we non-dimensionalize using $(\omega_0^*)^{-1}$ for time, $(g^* s/\omega_0^{*2})$ and $(g^* s^2/\omega_0^{*2})$ for the horizontal and vertical coordinates, respectively, and $(g^* s/\omega_0^*)$ for the velocity. With monochromatic incident waves, the cross-shore structure of the incident wave is described by J_0, the zero-order Bessel function of the first kind. Here, the dimensionless velocity potential ϕ_i of the incoming wave is assumed to be the superposition of a large number (N) of harmonic components of frequency f_n:

$$\phi_i = -a\frac{\mathrm{i}}{2}\sum_{n=1}^{N}\left(\frac{\mathcal{A}_n}{\omega_n} J_0(2\omega_n\sqrt{x})\mathrm{e}^{-\mathrm{i}\omega_n t}\right) + \text{c.c.} + O(a^2), \tag{2.2}$$

where $\omega_n = 2\pi f_n$, t is time, $\mathcal{A}_n$ is the complex amplitude (see Mei 1989 and Vittori & Blondeaux 1997 for more details) and c.c. denotes complex conjugate.

The spectrum is, by definition, narrow and energy is contained within an $O(a)$ band centred around ω_0^*. Therefore, the velocity potential of the wave field can be written as

$$\phi_i = -a\frac{\mathrm{i}}{2}\mathcal{A}(\tau)J_0(2\sqrt{x})\mathrm{e}^{-\mathrm{i}t} + \text{c.c.} + O(a^2), \tag{2.3}$$

where

$$\mathcal{A}(\tau) = \sum_{n=1}^{N} \mathcal{A}_n \mathrm{e}^{-\mathrm{i}\Omega_n \tau} = \sum_{n=1}^{N} \sqrt{2S(f_n)\Delta f}\,\mathrm{e}^{-\mathrm{i}(\Omega_n \tau - \psi_n)} \tag{2.4}$$

and

$$\Omega_n = \omega_n - 1 = 0(a). \tag{2.5}$$

The phases ψ_n are randomly and uniformly distributed between 0 and 2π. The incoming, narrow-band random wave has the cross-shore x structure of the centre frequency ω_0^*, with complex amplitude $\mathcal{A}$ modulated at the slow time scale $\tau = at$.

2.2. *Subharmonic edge waves*

The most unstable edge wave mode is described by the velocity potential ϕ_e (e.g. Mei 1989):

$$\phi_e = \epsilon\phi_0 = -\epsilon\frac{\mathrm{i}\mathcal{B}(\tau)}{\sigma}\mathrm{e}^{-kx}\cos(ky)\mathrm{e}^{-\mathrm{i}\sigma t} + \text{c.c.} \quad \text{with } \sigma^2 = k, \tag{2.6}$$

where the small parameter ϵ denotes the order of magnitude of the edge wave amplitude, y is the alongshore coordinate, k is the wavenumber, and $\mathcal{B}(\tau)$ describes the slow time growth of the standing edge wave amplitude.

3. Incident and edge wave interaction

3.1. *Monochromatic incident waves*

Energy transfer from incoming to subharmonic edge waves occurs at order ϵa, if the term proportional to $\mathrm{e}^{\mathrm{i}[\pm(1\pm\sigma)t]}$ is equal or close to $\mathrm{e}^{\pm\mathrm{i}\sigma}$ (i.e. when $\sigma \sim \pm 1/2$). Further terms proportional to $\mathrm{e}^{\pm\mathrm{i}\sigma}$ are generated at order ϵ^3 by the nonlinear self-interaction of the edge waves (radiation to the far field) and by the detuning. These further terms limit edge wave growth. Hence, a finite amplitude edge wave is found if $\epsilon = a^{1/2}$ and the velocity potential ϕ is expanded in the form

$$\phi = a^{1/2}\phi_0(x, y, \tau)\mathrm{e}^{-\mathrm{i}\sigma t} + a\phi_1(x, y, \tau)\mathrm{e}^{-2\mathrm{i}\sigma t} + a^{3/2}\phi_2(x, y, \tau)\mathrm{e}^{-\mathrm{i}\sigma t} + \text{c.c.} + \cdots, \tag{3.1}$$

where

$$\sigma = \tfrac{1}{2}(1 + a\mu) \tag{3.2}$$

and μ is a dimensionless detuning parameter such that the term $a(\mu/2)$ facilitates consideration of an edge wave with period of almost twice that of the incoming wave.

At order $a^{1/2}$, ϕ_0 is provided by (2.6). The solution of the problem at order a can be written as the sum of two terms:

$$\phi_1 = \phi_{1h} + \phi_{1p}, \tag{3.3}$$

where ϕ_{1h} is the solution of the homogeneous equation

$$\phi_{1h} = -\frac{\mathrm{i}}{2}\mathcal{A}(\tau)J_0(2\sqrt{x}) \tag{3.4}$$

that describes the incoming wave, and ϕ_{1p} is a particular solution

$$\phi_{1p} = \mathrm{i}2\pi\sigma\mathcal{B}^2(\tau)G(kx) \tag{3.5}$$

that describes nonlinear effects on the edge wave time development. The function G satisfies

$$kx\frac{\mathrm{d}^2G(kx)}{\mathrm{d}(kx)^2} + \frac{\mathrm{d}G(kx)}{\mathrm{d}(kx)} + 4G(kx) = \frac{\mathrm{e}^{-2kx}}{\pi} \tag{3.6}$$

and is given by

$$G(kx) = -E_2(kx)J_0(4\sqrt{kx}) + E_1(kx)Y_0(4\sqrt{kx}) + [E_2(\infty) - \mathrm{i}E_1(\infty)]J_0(4\sqrt{kx}), \tag{3.7}$$

with

$$E_1(kx) = \int_0^{kx} \mathrm{e}^{-2\chi}J_0(4\sqrt{\chi})\,\mathrm{d}\chi, \quad E_2(kx) = \int_0^{kx} \mathrm{e}^{-2\chi}Y_0(4\sqrt{\chi})\,\mathrm{d}\chi. \tag{3.8a,b}$$

At order $a^{3/2}$ terms proportional to $\cos(ky)\mathrm{e}^{\pm\mathrm{i}\sigma t}$ arise from the nonlinear interactions between the edge wave and incoming wave, and from the nonlinear self-interaction of the edge wave. Hence ϕ_2 (see (3.1)) has the form:

$$\phi_2 = H(x,\tau)\cos(ky). \tag{3.9}$$

The equation for H is

$$\sigma^2 H + \left[\frac{\mathrm{d}}{\mathrm{d}x}\left(x\frac{\mathrm{d}H}{\mathrm{d}x}\right) - k^2xH\right] = -3\mathrm{i}\frac{k^4}{\sigma^3}\mathcal{B}^2\overline{\mathcal{B}}\mathrm{e}^{-3kx} + \left[-2\frac{\partial\mathcal{B}}{\partial\tau} + \mathrm{i}\frac{\overline{\mathcal{B}}}{4\sigma}\left(2k\frac{\mathrm{d}J_0}{\mathrm{d}x} + \frac{\mathrm{d}^2J_0}{\mathrm{d}x^2}\right) - \mathrm{i}\frac{2\pi k}{\sigma}\overline{\mathcal{B}}\mathcal{B}^2\left(2k\frac{\mathrm{d}G}{\mathrm{d}x} + \frac{\mathrm{d}^2G}{\mathrm{d}x^2}\right)\right]\mathrm{e}^{-kx} = P(x). \tag{3.10}$$

The homogeneous problem for H has the non-trivial solution e^{-kx} and the solvability condition (Fredholm alternative) yields

$$\int_0^{\infty} \mathrm{e}^{-kx}P(x)\,\mathrm{d}x = 0. \tag{3.11}$$

A significant amount of algebra provides the evolution equation for $\mathcal{B}$:

$$\frac{\mathrm{d}\mathcal{B}}{\mathrm{d}\tau} = \frac{\mathrm{i}\mathcal{A}\tilde{\mathcal{B}}k^2}{4\sigma}\mathrm{e}^{-\mathrm{i}\mu\tau}\alpha - \left(\frac{\mathrm{i}2\pi k^3}{\sigma}\beta + \frac{\mathrm{i}3k^4}{4\sigma^3}\right)\tilde{\mathcal{B}}\mathcal{B}^2, \tag{3.12}$$

where $\alpha = 0.541$, $\beta = -0.0894 - 0.0366\mathrm{i}$, and $\tilde{\mathcal{B}}$ is the complex conjugate of $\mathcal{B}$ (Li 2007). Equation (3.12) is reduced to the amplitude equation by Li (2007), if monochromatic forcing ($\mathcal{A}(\tau) = 1$) and only perfect resonance are considered ($\mu = 0$).

With a monochromatic wave ($\mathcal{A}(\tau) = 1$), perfect resonance ($\mu = 0$), and assuming that $\mathcal{B}$ is small during the initial edge wave growth, the cubic terms are negligible and (3.12) yields

$$\mathcal{B}(\tau) = \mathcal{B}_0 \exp\left[\pm\frac{2k^2}{\sigma}E_1(\infty)\tau\right] \quad \text{with } E_1(\infty) = \frac{\alpha}{8}. \tag{3.13}$$

As the amplitude of the edge wave $\mathcal{B}$ grows, cubic terms become significant and limit edge wave growth to an equilibrium amplitude ($\mathcal{B}_\infty$) that follows from (3.12) by considering $\mathrm{d}\mathcal{B}_\infty/\mathrm{d}\tau = 0$:

$$|\mathcal{B}_\infty| = \sqrt{\frac{8E_1(\infty)}{\left|16\pi E_G - \frac{5}{4}\right|}} \simeq 1.35 \quad \text{with } E_G = \int_0^\infty \mathrm{e}^{-2\xi}G(\xi)\,\mathrm{d}\xi = 0.02862 - 0.004578\mathrm{i}. \tag{3.14}$$

Detuning from perfect resonance (i.e. $\sigma \neq 1/2$), $\mathcal{C} = \mathcal{B}\mathrm{e}^{\mathrm{i}(\mu/2)\tau}$ transforms equation (3.12) to a constant coefficient equation

$$\frac{\partial \mathcal{C}}{\partial \tau} = \mathrm{i}\alpha\frac{k^2}{4\sigma}\mathcal{A}\tilde{\mathcal{C}} + \mathrm{i}\frac{\mu}{2}\mathcal{C} - \frac{\mathrm{i}k^3}{\sigma}\left(2\pi\beta + \frac{3}{4}\right)\tilde{\mathcal{C}}\mathcal{C}^2. \tag{3.15}$$

The first right-hand-side term of (3.15) relates edge wave amplitude changes ($\partial\mathcal{C}/\partial\tau$) to energy transfer from/to the incoming wave. The second term is detuning (deviations from perfect resonance). The third term describes nonlinear effects that limit edge wave growth: radiation of edge wave energy towards offshore, and detuning. Figure 1 shows the time development of $|\mathcal{B}|$ for different values of the detuning parameter μ. The largest values of $\mathcal{B}_\infty$ are off-resonance for σ larger than 0.5, one aspect of the complicated hysteresis and bifurcations that can occur with idealized, monochromatic waves (e.g. Li & Mei 2007).

To include damping effects due to the bottom boundary layer, Guza & Davis (1974) estimated the time-averaged energy dissipation rate per unit area as $D^* = \overline{\tau_x^* U^* + \tau_y^* V^*}$, where an overbar indicates time average and τ_x^* and τ_y^* are the horizontal components of the bottom shear stress (U^* and V^* being the corresponding velocity components). Assuming a laminar boundary layer

$$D^* = \frac{\rho^* \nu^*}{2\delta^{*2}}\overline{(|U^*|^2 + |V^*|^2)}. \tag{3.16}$$

In (3.16), ρ^* denotes the density of the water, ν^* is the kinematic viscosity and $\delta^* = \sqrt{2\nu^*/\omega_0^*}$ is the bottom boundary layer thickness. For mode $n = 0$, the integration of (3.16) both cross-shore and alongshore, leads to a viscous edge wave damping described by

$$\frac{\mathrm{d}\mathcal{B}}{\mathrm{d}t} = -\frac{\nu^*\omega_0^*}{8g^* s^2 \delta^*}\mathcal{B}. \tag{3.17}$$

Equation (3.17) can also be written as

$$\frac{\mathrm{d}\mathcal{B}}{\mathrm{d}\tau} = -\frac{\delta^*}{16a^*}\mathcal{B} = -R^L\mathcal{B}, \tag{3.18}$$

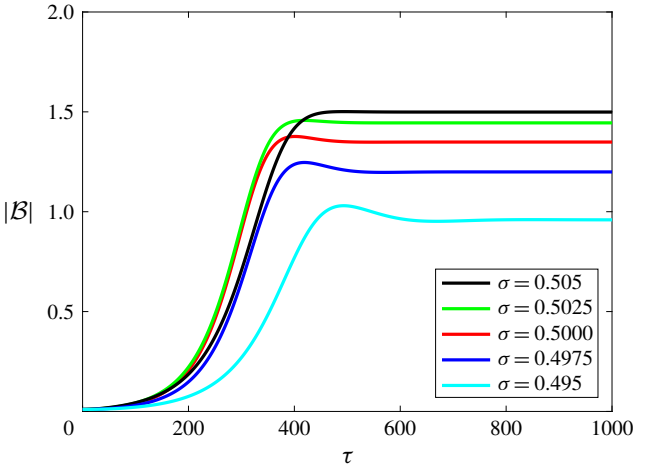

FIGURE 1. Dimensionless edge wave amplitude ($|\mathcal{B}|$) versus the slow time scale (τ) for monochromatic incident waves ($\mathcal{A} = 1$), small initial amplitude of the edge wave ($\mathcal{B}(0) = 0.01$), and: (1) red, no detuning ($\sigma = 0.5$); (2) other colours, non-zero detuning (see legend).

where R^L is the damping coefficient referring to an 'idealized' laminar boundary layer over a smooth bottom. In the field the bottom boundary layer is turbulent and the effect of the roughness cannot be neglected. The dissipation rate is expected to increase and the wave damping due to dissipative effects is computed by means of (3.18) with a damping coefficient R larger than R^L. A rough estimate of the order of magnitude of R can be obtained by considering the ratio between the thickness of the turbulent boundary layer and a^*. With the turbulent bottom boundary layer thickness of a few centimetres and wave amplitude of metres, $O(R) = 10^{-3}$.

Hence, the $\mathcal{C}$ evolution equation (3.15) is modified by adding the damping term $-R\mathcal{C}$:

$$\frac{\partial \mathcal{C}}{\partial \tau} = \mathrm{i}\alpha \frac{k^2}{4\sigma} \mathcal{A}\tilde{\mathcal{C}} + \left(\mathrm{i}\frac{\mu}{2} - R\right)\mathcal{C} - \frac{\mathrm{i}k^3}{\sigma}\left(2\pi\beta + \frac{3}{4}\right)\tilde{\mathcal{C}}\mathcal{C}^2. \tag{3.19}$$

3.2. *Random incident waves*

With random incident waves $\mathcal{A}$, equation (3.19) is solved numerically for $\mathcal{C}$ with a second-order Runge–Kutta scheme. For simplicity, assume a Gaussian incident energy spectrum S, characterized by standard deviation $a\sigma_e$:

$$S = \frac{\sqrt{\pi}}{2\sqrt{2}} \frac{a}{\sigma_e} \mathrm{e}^{-((\omega-1)/\sqrt{2}a\sigma_e)^2} = \frac{\sqrt{\pi}}{2\sqrt{2}} \frac{a}{\sigma_e} \mathrm{e}^{-(\Omega/\sqrt{2}\sigma_e)^2}, \tag{3.20}$$

with

$$\mathcal{A}(\tau) = \sum_{n=1}^{N} \sqrt{\frac{1}{2\sqrt{2\pi}} \frac{1}{\sigma_e} \mathrm{e}^{-\left(\Omega_n/\sqrt{2}\sigma_e\right)^2} \Delta\Omega} \mathrm{e}^{\mathrm{i}\psi_n} \mathrm{e}^{-\mathrm{i}\Omega_n \tau}. \tag{3.21}$$

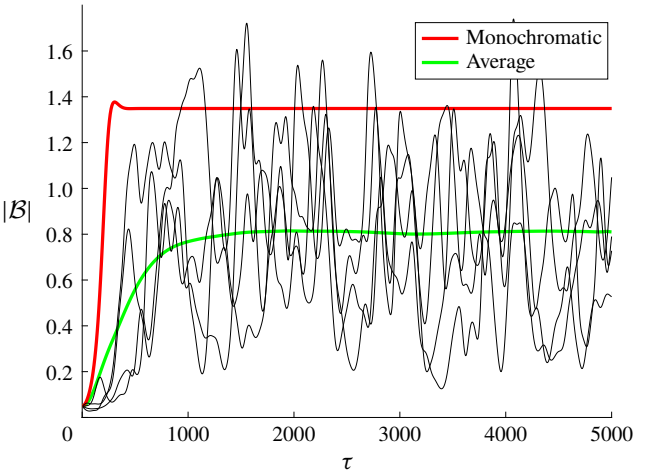

FIGURE 2. Edge wave amplitude ($|\mathcal{B}|$) versus the slow time scale τ for monochromatic (thick red curve), and four random realizations ($|\mathcal{B}_i|$, thin black lines). The ensemble-averaged edge wave amplitude with $M = 1000$ is also plotted (thick green line). Parameters: $a = 0.2$, $\sigma = 0.5$ $(\mu = 0)$, $R = 0$, $\sigma_e = 0.02$, $N = 30\,000$ and $|\mathcal{B}(0)| = 0.05$.

For each realization, ψ_n are a set of random phases. The value of $\mathcal{B}$ is ensemble averaged over many (M) realizations:

$$\langle|\mathcal{B}|\rangle = \lim_{M\to\infty} \frac{1}{M} \sum_{i=1}^{M} |\mathcal{B}_i|. \tag{3.22}$$

4. Results

Randomness of the incident wave significantly reduced the ensemble-averaged subharmonic edge wave amplitude $\langle\mathcal{B}\rangle$ from the monochromatic wave $|\mathcal{B}|_\infty = 1.35$ (figure 2). The quantitative value of the reduction depends on the values of the parameters a, σ and σ_e. Results for different incoming wave spectral widths σ_e and detuning μ show that $\langle|\mathcal{B}|_\infty\rangle$ is maximum for the narrowest spectrum (smallest σ_e). Moreover, the maximum of $\langle|\mathcal{B}|_\infty\rangle$ is found for small positive values of μ thus indicating that a small positive detuning increases the equilibrium amplitude attained by the edge waves (figure 3). As σ_e increases, the frequency range of excitable edge waves increases but the ensemble amplitude $\langle|\mathcal{B}|\rangle$ decreases (figure 3). The unstable equilibrium points of the amplitude equations and hysteresis phenomenon of the monochromatic case (e.g. Blondeaux & Vittori 1995 and references therein) are suppressed with random waves. Finally, increasing viscous effects decreases both $|\mathcal{B}|$, and the range of σ where edge waves form (figure 4). Indeed, for large R, viscous damping suppresses edge wave growth, as with monochromatic incident waves (figure 5).

5. Discussion and conclusions

A monochromatic surface gravity wave, normally incident on and strongly reflected at a sloping beach, is unstable to perturbation by subharmonic edge waves. The edge

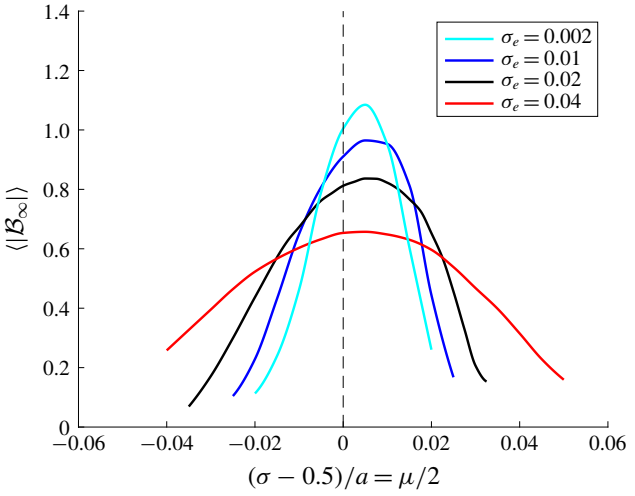

FIGURE 3. Equilibrium ensemble-averaged edge wave amplitude ($\langle|\mathcal{B}|_\infty\rangle$) versus deviation from exact resonance for different values of σ_e (see legend). Parameters: $|\mathcal{B}(0)| = 0.05$, $a = 0.2$, $R = 0$, $N = 30\,000$, $M = 200$. For a monochromatic incident wave ($\sigma_e = 0$)$|\mathcal{B}|_\infty$ is equal to 1.35 (see red curve in figure 2).

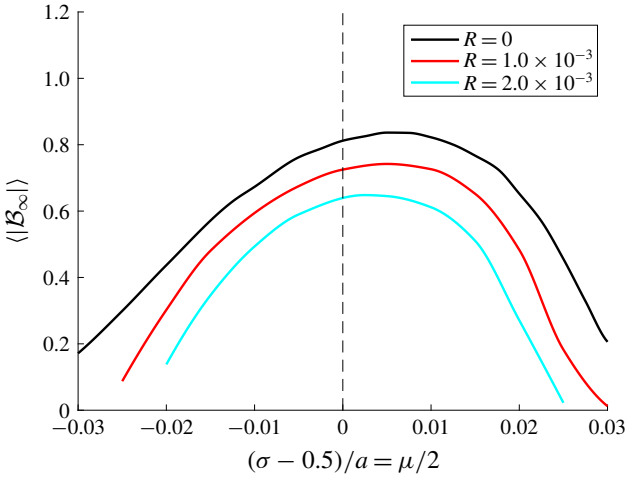

FIGURE 4. Equilibrium ensemble-averaged edge wave amplitude ($|\mathcal{B}|_\infty$) versus deviation from exact resonance for a random incoming wave and different R (see legend). Parameters: $|\mathcal{B}(0)| = 0.05$, $a = 0.2$, $\sigma_e = 0.02$, $N = 30\,000$, $M = 200$.

wave amplitudes grow relatively large (larger than the incident waves at the shoreline) until limited by nonlinear processes. The randomness of the incoming wave weakens the resonance, and can prevent the subharmonic edge wave amplitude from reaching the values attained with monochromatic incoming waves (figure 2). Phase differences between edge and incident waves, driven by randomness in incident waves, can reverse the usual energy flux (from incident waves to edge waves).

To illustrate the phenomenon, let us consider perfect resonance (i.e. $\sigma = 1/2$, $\mu = 0$) and neglect dissipative effects and the nonlinear terms. Then, equation (3.19) yields

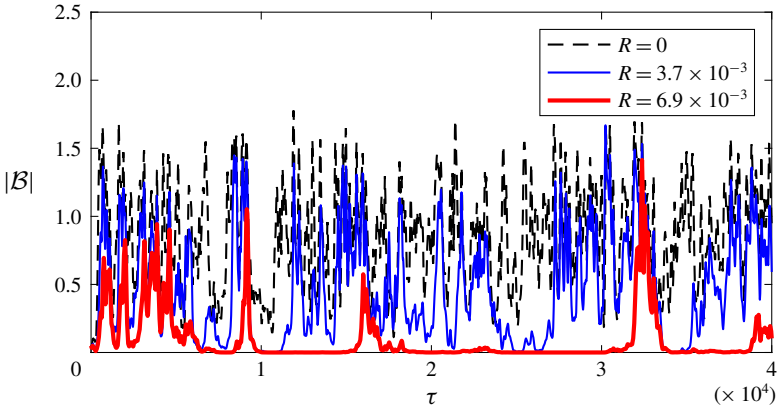

FIGURE 5. Dimensionless edge wave amplitude ($|\mathcal{B}|$) versus the slow time scale τ for one realization of the random incoming wave ($a = 0.2$, $\sigma = 0.5$, $\sigma_e = 0.02$, $\mathcal{B}(0) = 0.05$, $N = 30\,000$) and different R values. For a monochromatic incident waves and $R = 0$, $|\mathcal{B}|_\infty$ is equal to 1.35 (red curve in figure 2).

schematically

$$\frac{\partial \mathcal{C}}{\partial \mathcal{T}} = \mathrm{i}\mathcal{A}\tilde{\mathcal{C}}, \tag{5.1}$$

where $\mathcal{T}$ is a modified temporal scale ($\mathcal{T} = \alpha k^2/4\sigma$).

By substituting $\mathcal{C} = |\mathcal{C}|\mathrm{e}^{\mathrm{i}\theta}$ and $\mathcal{A} = |\mathcal{A}|\mathrm{e}^{\mathrm{i}\varphi}$, one obtains

$$\frac{\mathrm{d}|\mathcal{C}|}{\mathrm{d}\mathcal{T}} = |\mathcal{A}||\mathcal{C}|\sin(2\theta - \varphi), \quad \frac{\mathrm{d}\theta}{\mathrm{d}\mathcal{T}} = |\mathcal{A}|\cos(2\theta - \varphi), \tag{5.2a,b}$$

thus showing that the edge wave growth/decay depends on the difference between the edge and incident wave phases 2θ and φ. Edge wave perturbations such that $2\theta - \varphi$ is equal to $\pi/2$ have the most rapid (exponential) growth. Eventually, growth is limited by the nonlinear terms which are neglected in (5.1). However, with random incident waves, $(2\theta - \varphi)$ varies between 0 and 2π over group time scales. When $(2\theta - \varphi) = 3/2\pi$, the energy flux from quadratic interactions between incident and edge waves is reversed. Of course, edge wave amplitude evolution is also influenced by cubic nonlinear terms and friction terms (see figure 2 and (3.19)). The effects of the bottom friction reduce the amplitude of the edge waves that form. The combined action of the phase difference and of large friction effects causes the prediction of an intermittent subharmonic edge wave excitation, depending on the values of the parameters. With $R = 3.7 \times 10^{-3}$ (blue line in figure 5), edge wave amplitudes vary between near zero and near $\mathcal{B} = 1.35$, the value observed with monochromatic incident waves. With $R = 6.9 \times 10^{-3}$, edge waves occur only for a relatively short time (red curve in figure 5).

The requirement of $a \ll 1$ has implications for the applicability to oceanic waves. Assuming $a = 0.2$ (as in the figures), a range of combinations is possible (e.g. beach slope 0.1, wave period and amplitude 12 s and 0.16 m, respectively) but if the beach slope is not steep (e.g. 0.05), the wave conditions necessary to satisfy $a = 0.2$ are rarely encountered (e.g. for a wave period of 12 s, the corresponding wave height

is 0.02 m). Indeed, while in the laboratory transient subharmonic edge waves were observed (Ding *et al.* 2018), they could be difficult to detect in the field, given the background level of waves at all frequencies.

To conclude, the analysis previously described shows that the edge wave amplitude varies on time scales similar to incident wave groups, and responds to variations in both incident wave phase and amplitude. With bottom friction included, intermittent subharmonic edge wave excitation is predicted. Edge wave amplitudes can vary between near zero and the relatively large amplitudes observed with monochromatic incident waves.

Acknowledgements

R.T.G. was supported by the United States Army Corps of Engineers Coastal Ocean Data Systems Program (W912HZ-14-2-0025), and the California Department of Parks and Recreation, Division of Boating and Waterways Oceanography Program (C1370032).

References

ABCHA, N., ZHANG, T., EZERSKY, A., PELINOVSKY, E. & DIDENKULOVA, I. 2017 Subharmonic resonant excitation of edge waves by breaking surface waves. *Nonlinear Process. Geophys.* **24** (2), 157–165.

BLONDEAUX, P. & VITTORI, G. 1995 The nonlinear excitation of synchronous edge waves by a monochromatic wave normally approaching a plane beach. *J. Fluid Mech.* **301**, 251–268.

BRICKER, J. D., MUNGER, S., PEQUIGNET, C., WELLS, J. R., PAWLAK, G. & CHEUNG, K. F. 2007 ADCP observations of edge waves off Oahu in the wake of the November 2006 Kuril islands tsunami. *Geophys. Res. Lett.* **34** (23), L23617.

BUCHAN, S. J. & PRITCHARD, W. G. 1995 Experimental observations of edge waves. *J. Fluid Mech.* **288**, 1–35.

CARRIER, G. F. & GREENSPAN, H. P. 1958 Water waves of finite amplitude on a sloping beach. *J. Fluid Mech.* **4** (1), 97–109.

DING, X., COCO, G., GUZA, R. T., GARNIER, R., WHITTAKER, C., DALRYMPLE, R., WEI, Z., BLANCO, B., LO MONACO, P., BLONDEAUX, P. *et al.* 2018 Intermittent subharmonic edge wave excitation with random incoming waves. *Abstract, AGU Fall Meeting*. AGU.

GALLAGHER, B. 1971 Generation of surf beat by non-linear wave interactions. *J. Fluid Mech.* **49** (1), 1–20.

GALVIN, C. J. 1965 Resonant edge waves on laboratory beaches. *EOS Trans. Am. Geophys. Union* **46**, 112.

GREENSPAN, H. P. 1956 The generation of edge waves by moving pressure distributions. *J. Fluid Mech.* **1** (6), 574–592.

GUZA, R. T. & BOWEN, A. J. 1976 Finite-amplitude edge waves. *J. Mar. Res.* **34** (2), 269–293.

GUZA, R. T. & DAVIS, R. E. 1974 Excitation of edge waves by waves incident on a beach. *J. Geophys. Res.* **79** (9), 1285–1291.

GUZA, R. T. & INMAN, D. L. 1975 Edge waves and beach cusps. *J. Geophys. Res.* **80** (21), 2997–3012.

HARRIS, T. F. W. 1967 Field and model studies of the nearshore circulation. PhD dissertation, University of Natal, South Africa.

JOHNSON, R. S. 2005 Some contributions to the theory of edge waves. *J. Fluid Mech.* **524**, 81–97.

LI, G. 2007 Nonlinear resonance of trapped waves on a plane beach. PhD thesis, Massachusetts Institute of Technology.

LI, Y. & MEI, C. C. 2007 Subharmonic resonance of a trapped wave near a vertical cylinder by narrow-banded random incident waves. *J. Engng Maths* **58** (1–4), 157–166.

MEI, C. C. 1989 *The Applied Dynamics of Ocean Surface Waves*. World Scientific.

MINZONI, A. A. & WHITHAM, G. B. 1977 On the excitation of edge waves on beaches. *J. Fluid Mech.* **79** (2), 273–287.

MUNK, W., SNODGRASS, F. & CARRIER, G. 1956 Edge waves on the continental shelf. *Science* **123** (3187), 127–132.

ROCKLIFF, N. 1978 Finite amplitude effects in free and forced edge waves. *Math. Proc. Camb. Phil. Soc.*, **83** (3), 463–479.

VITTORI, G. & BLONDEAUX, P. 1997 Edge wave excitation by random sea waves. In *Proceedings of the 27th International Association of Hydraulic Research (San Francisco, CA, August 1997)*, pp. 16–21. ASCE.

YEH, H. H. 1986 Experimental study of standing edge waves. *J. Fluid Mech.* **168**, 291–304.